EVALUATION OF THE MODE II CRITICAL ENERGY RELEASE RATE UNDER IMPACT FOR THERMOPLASTIC COMPOSITE LAMINATE USING INFRARED THERMOGRAPHY

Garcia Pérez P.[1*], Dau F.[1], Bouvet C.[2], Ballère L.[3] and Peres P.[3]
[1] Arts et Métiers ParisTech, Institut de Mécanique et d'Ingénierie, UMR CNRS 5295
Talence, France
[2] ISAE Supaéro, Institut Clément Ader, Toulouse, France
[3]Airbus Safran Launchers, Saint-Médard-en-Jalles, France
* Corresponding author (pablo.garcia-perez@ensam.eu)

Keywords*: composite damage, thermography, numerical simulation*

ABSTRACT

Composite materials have increasingly been used in aerospace applications because of their advantageous specific mechanical properties. Nevertheless, impact damage leads to significant reduction in structure compressive strength though damage may remain unnoticed. Currently, there is a strong trend towards a greater use of high-performance thermoplastics. They present a great impact energy absorption, good delamination resistance and great residual strength after impact.

In previous work, a finite element model was used to simulate impact and compression after impact tests. The proposed model demonstrated a significant ability to predict the low-velocity impact behavior of carbon fiber reinforced thermoplastic resin (CFRTP) composite laminates. However, it showed an important sensitivity to the critical energy release rate in mode II, G_{IIC}.

In the present study, the Short Beam Shear (SBS) test was chosen to further investigate G_{IIC} using a CFRTP laminate with a stacking sequence of $[0_2/90_4/0_2]$. SBS test was previously used to study permanent indentation. It allows maximizing the induced shear stress causing the opening of matrix cracks that have a precursor role in delamination growth. Mode II interlaminar delamination is promoted by the shear stress state. Infrared thermography was used to study the dissipative phenomena at the crack tip during delamination propagation. The goal was to link the critical energy release rate in mode II, G_{IIC} to the experimental heat sources measured experimentally. SBS test also allowed for investigating the relationship between intra-ply damage (matrix cracks) and inter-ply damage (delamination).

1 INTRODUCTION

The use of composite materials is quickly growing in aerospace and automotive industries applications. However, impact damage in composite structures may lead to significant reduction in structural compressive strength and this damage may remain unnoticed below the Barely Visible Impact Damage threshold. Damage in composite materials and structures involves multiple failure modes such as fiber breakage, fiber pull-out, delamination between plies, matrix cracking, fiber-matrix debonding, etc.

High-performance thermoplastic composites display a better resistance to impact damage. In the present study, a carbon fiber reinforced thermoplastic (CFRTP) composite unidirectional laminate is considered. It presents inherently non-linear material properties with greater residual strength after impact, higher toughness, better delamination resistance and can absorb a greater quantity of energy in impact and crash than using carbon fiber reinforced thermosetting composite [1].

The impact fracture process is quite complex. It involves several types of damage directly influencing the response of the laminate composite material. The extent of each failure mode may vary from ply to ply depending on the stacking sequence and loading direction. The first type of damage to appear is the matrix failure in the region of high stress gradients. Matrix cracking has been widely reported as the first type of failure induced by transverse low velocity impact. The matrix being damaged, the loads are transferred to the ply with fiber orientation aligned close to the applied load direction. The fiber-matrix interfaces are fractured in these plies. This is accompanied by the fracture of the fibers. Due to the coupling between matrix cracking and delamination, the initiation of delamination will occur at the location where the matrix cracks reaches the interface. Delamination always occurs at the interfaces between plies with different fiber orientations. Delamination propagation is driven mostly in mode II and it is considered to be the most energy-consuming damage mechanism during the impact event.

Many experimental techniques are used to explain the failure damage chronology, to characterize material properties and to test impact resistance of unidirectional composite materials. However, experiments are expensive, time-consuming and limited to several configurations. That is why computational methods are developed in order to reproduce impact damage and predict impact resistance.

Impact damage behavior is very difficult to model because it depends on many parameters that have to be identified experimentally. Delamination is the most critical damage in impact and its propagation is driven mostly in mode II. It is usually modeled using cohesive interface elements based on fracture mechanics. The bilinear cohesive law needs three parameters: the initial interface stiffness K, the critical stress σ_C and the critical energy release rate G_C. In previous authors work, a finite element model was used to simulate impact and compression after impact tests with good results [2][3]. Nevertheless, it showed an important sensitivity to the critical energy release rate in mode II, G_{IIC} [4]. To develop relevant models to predict such a failure, particular attention should be given to the determination of G_{IIC}.

There are several tests in the literature allowing the study of mode II delamination. The Iosipescu test and the Modified Rail Shear subject the structure to shear stress, but they are mainly performed to investigate the initiation of the delamination. In addition, they require complex test setup and a thick specimen. This induces a structural effect and does not allow for proper determining the intrinsic material property.

The End-Notched Flexure, the Four point End-Notched Flexure and the End Loaded Split are the most commonly-used tests to measure the mode II fracture properties. The ENF test has been the most used because of the simple setup [5] but G_{IIC} results show a considerable scatter for carbon fiber/thermoplastic composite. Used to study 0°/0° interfaces delamination for CFRTP, it exhibited G_{IIC} values varying from 0.4 N/mm to 2.3 N/mm [6][7]. Used as well to study G_{IIC} for carbon/epoxy multidirectional laminates, G_{IIC} values increased with the ply angle 0°/θ° from 0.7 N/mm to 1.4N/mm [8]. In addition, loading strain rate influences the interface toughness: carbon/PEEK APC-2 exhibits ductile crack growth at low rates and brittle crack growth at high rates [9][10]. When crack growth velocity increases, G_{IIC} decreases from 1.4 to 0.4 N/mm. Finally, ENF test can induce unstable propagations [8][11], associated with high velocity of crack growth.

The goal of this paper is to propose a test reproducing the impact configuration (out-of-plane loading) and impact damage chronology (matrix cracking followed by unstable mode II delamination propagation). Standard tests need the presence of an initial crack in the mid-plane of the beam, which is not the case in impact scenario. Short Beam Shear (SBS) test, previously used to study the permanent indentation [12], is chosen in the present study to further investigate G_{IIC} value in unidirectional prepreg laminate made of carbon fiber and thermoplastic resin. This test allows to minimize the flexural (tensile and compressive) stresses and to maximize the induced shear stresses. It causes the opening of matrix cracks that have a precursor role in delamination development. Unstable mode II delamination propagation is promoted by the shear stress state.

Compliance method used in ENF tests for G_{IIC} calculation is inaccurate for unstable propagation. Infrared thermography technique is preferred in this study to evaluate G_{IIC} using the heat energy dissipated by the crack growth. This technique allows for local measuring of fracture toughness in unclassical tests. Infrared thermography was used to calculate the energy release rate associated with transverse weft cracking [13] and fracture toughness of compressive fiber failure [14] leading to promising results.

2 SHORT BEAM SHEAR TEST

The geometry of the device is given in Figure 1. The plate was simply supported on two cylinders of 6 mm diameter and the force was imposed at the center using a 12 mm diameter cylinder. Specimens with a dimension of 30 x 10 x 1.3 mm^3 were made of CFRTP laminate with a stacking sequence of $[0_2/90_4/0_2]$.

The goal was to generate matrix cracking in the 90° plies due to shear stresses, followed by delamination in the 0°/90° plies interface. Before delamination appears, stress concentration under the upper cylinder can lead to compressive fiber failure of 0° upper ply. Several setups were tested until the final configuration was chosen in order to promote impact damage chronology (matrix cracking followed by delamination). The span (distance between the two lower cylinders) to thickness ratio (s/t) should be reduced [15]. The span was set to 8 mm and the span to thickness ratio was set to 6. Digital image correlation was used to validate the shear strain state in the center of the specimen.

In order to study the effect of loading velocity, quasi-static (0.2-0.6 mm/s) and dynamic (1.2 m/s) tests were carried out. A Nistron universal testing machine was used for quasi-static tests. Displacement rate is imposed by the machine and force was measured by the machine force cell. Dynamic tests were performed using a drop tower with

a 0.545 kg impactor. The initial impact velocity was acquired thanks to an optical laser system. Contact force during the impact was measured by a piezoelectric force sensor placed inside the impactor. The level of energy in the dynamic test was set to be the same as the quasi-static test. The result of eight quasi-static tests (S1-S8) and four dynamic tests (D1-D4) are presented below.

In quasi-static tests, a linear response was obtained in the first part of the loading (Figure 2). Then, damage occurred in two different ways. In the first case, every damage mode (matrix cracking, delamination and lastly fiber breaking) appeared instantly, causing the sudden failure of the sample (S3). In the second case, only matrix cracking and delamination were activated, and the force-displacement curve shows a progressive degradation of the sample, with several load drops linked to damage propagation (S2 sample). Both tests (quasi-static and dynamic) showed a good reproducibility in terms of maximum force/displacement. The same damage chronology is found in both cases and crack growth is unstable no matter the loading rate.

Usually matrix cracks propagate vertically or at a 45° direction in carbon fiber/epoxy laminates under loading. In the present thermoplastic laminate, matrix cracking followed a stair trajectory in the 90_4 ply. It started as a 45° direction matrix crack and then bifurcated into a 90°/90° interface delamination (Figure 3). A crack follows the trajectory that minimizes energy consumption and delamination between 90° plies seems to be less energy-consuming than directly crossing the 90°ply through the thickness.

Once the matrix crack reached the interface between 0° and 90° plies, delamination propagation occurred. It was unstable in every sample tested (quasi-static and dynamic). A high speed camera (Photron SA5) was used to estimate crack propagation speed during tests. This was not possible due to the weak dimensions of the sample and camera limitations (insufficient spatial and time resolution).

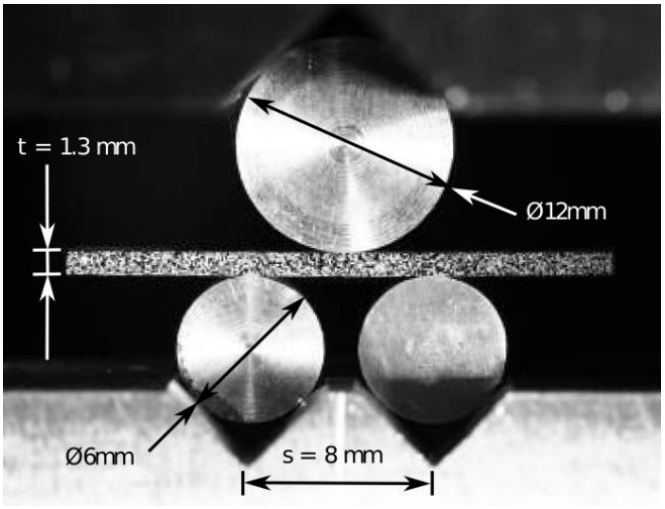

Figure 1 Short Beam Shear test setup

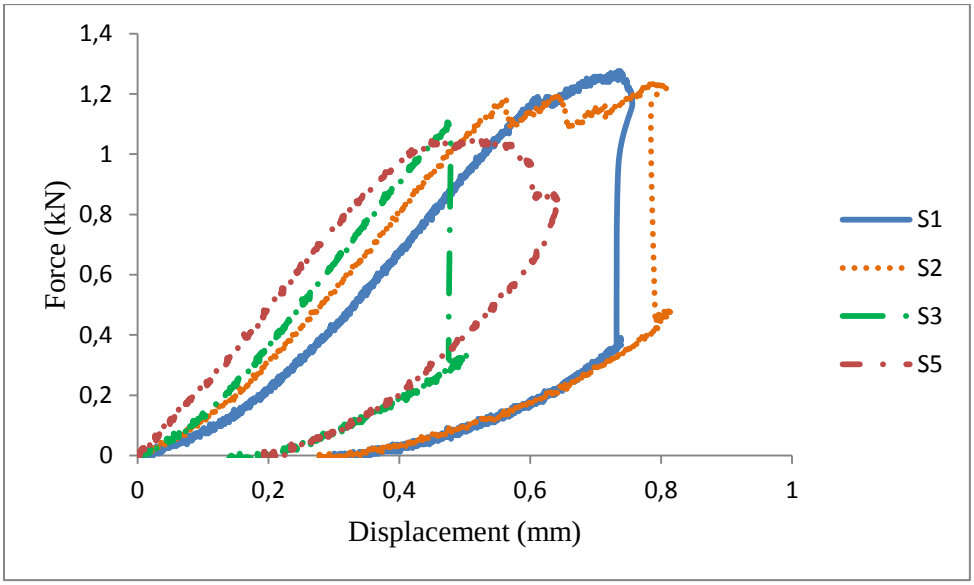

Figure 2 Force-displacement curve of the SBS quasi-static tests S1, S2, S3 and S5

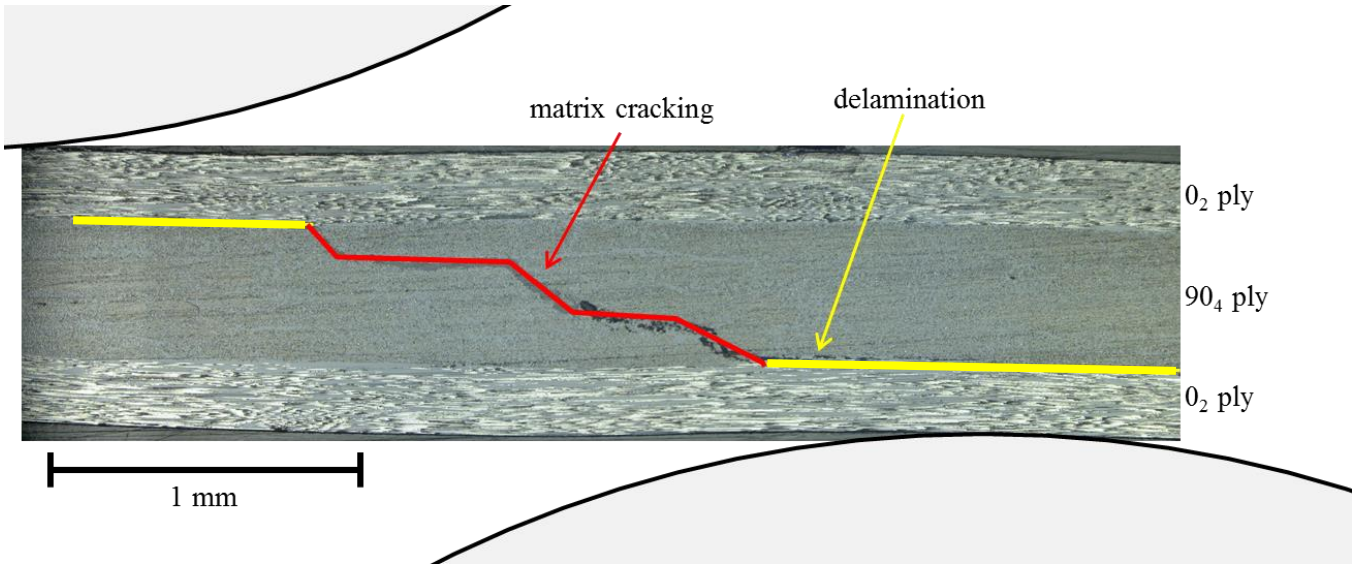

Figure 3 Post-mortem micrography of the S4 sample showing stair-fashion matrix crack and delamination

3 EVALUATION OF G_{IIC} USING INFRARED THERMOGRAPHY

Every test was operated at room temperature (293 K) and tracked with an infrared camera (FLIR SC700 MW) to monitor the thermal response. The infrared camera has a maximum resolution of 320 x 256 pixels^2 and a thermal resolution of 0.025 K for relative temperature measurement. The spatial resolution was set at 0.03 mm/pixel. Thermal images were recorded at a frequency varying from 380 Hz to 2176 Hz (used in dynamic tests). A thermal image of the initial setup of the SBS test is shown in Figure 4.

Delamination crack growth is a very fast phenomenon since the propagation in this material is highly unstable, even for quasi-static loading. Once the crack propagated, it induced an important rise of the temperature, from 23°C to 31°C in the crack tip. The heat energy dissipation after the crack passing is a slow phenomenon and can be evaluated with the infrared camera.

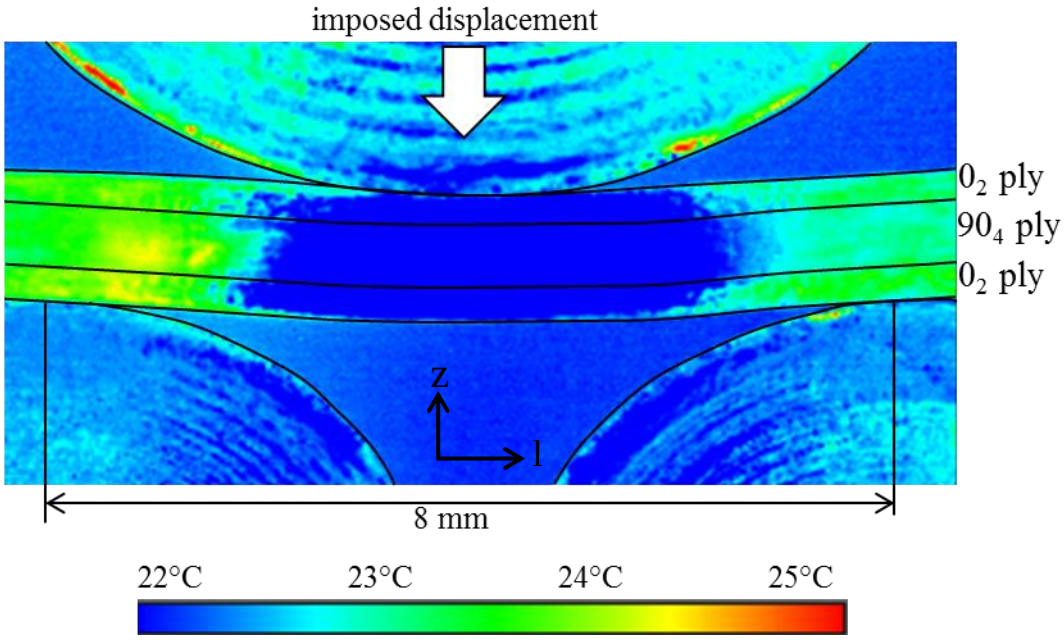

Figure 4 Temperature field at the start of the SBS test

The concept of infrared thermography is based on thermo-mechanical background. The full details can be found in [13][14]. The principle is to use heat diffusion equation to evaluate the intrinsic dissipation of the damaged material. Left term of the heat diffusion equation can be evaluated using spatial and temporal data provided by the infrared camera:

$$\rho C \frac{d\theta}{dt} - \left(k_{ll} \frac{\partial^2 \theta}{\partial l^2} + k_{tt} \frac{\partial^2 \theta}{\partial t^2} + k_{zz} \frac{\partial^2 \theta}{\partial z^2} \right) = \phi_{int} + s_{\text{the}} \quad (1)$$

where ρ is the mass density, C the specific heat capacity, $\theta = T - T_0$ the temperature variation between the current state and the initial equilibrium state T_0, k_{ll} (k_{tt}, k_{zz}) the conductivity in l (t, z) direction, ϕ_{int} the intrinsic dissipation and s_{the} the thermo-mechanical coupling. Properties of the CFRTP laminate can be found in Table 1.The thermo-

mechanical coupling can be neglected compared to intrinsic dissipation ($s_{the} << \phi_{int}$). Moreover the irreversible dissipation ϕ_{irrev}, which is necessary to evaluate the G_{IIC}, can be separated into two parts; the intrinsic dissipation ϕ_{int} evaluated using infrared thermography and the stored energy ϕ_{stored}:

$$\phi_{irrev}=\phi_{int}+\phi_{stored} \tag{2}$$

The stored energy is very difficult to evaluate and the Taylor-Quinney coefficient [27] is needed. This coefficient denotes the ratio of energy dissipated as heat, the intrinsic dissipation, dW_{diss}, to irreversible energy, dW_{irrev}:

$$\beta = \frac{\int_{t_A}^{t_{A+dA}} \int_{\Omega_{fis}} \phi_{int}.dV.dt}{\int_{t_A}^{t_{A+dA}} \int_{\Omega_{fis}} \phi_{irrev}.dV.dt} \approx \frac{dW_{diss}}{dW_{irrev}} \tag{3}$$

More precisely, the Taylor-Quinney coefficient [16] is defined as the ratio of the integrals over time and space of the intrinsic dissipation, dW_{diss}, and of the irreversible energy, dW_{irrev}, where t_A (t_{A+dA}) denotes the time for which the crack area is A (A+dA) and Ω_{fis} a volume containing the crack. Taylor-Quinney coefficient values vary from 0 to 1.If all the dissipated energy is converted into heat, β is equal to 1. This coefficient depends on different parameters, such as the strain level, the strain rate and the damage mechanisms involved. If the fracture is brittle (unstable crack growth), β is close to 1 and if the fracture mode is ductile (stable crack growth), β has a lower value. Given that it is difficult to precisely evaluate β and that crack propagation is highly unstable in the material studied, β was supposed equal to 0.9 in this work. Using the dissipated energy evaluated with the infrared thermography it is possible to evaluate then G_{IIC}:

$$G_{IIC} = \frac{dW_{irrev}}{dA} = \frac{dW_{diss}}{\beta.dA} \tag{4}$$

This method does not allow for the separation of the fracture modes (I, II or III), but only to evaluate the total critical energy release rate, and an additional study is necessary to extract the critical release rate from the different modes. SBS tests were used because it promotes mode II delamination propagation.

Young's modulus in fiber direction, E_l	150 GPa
Thermal conductivity in fiber direction, k_{ll}	5.4 $W.m^{-1}.K^{-1}$
Thermal conductivity in transverse direction, k_{tt} and k_{zz}	0.25 $W.m^{-1}.K^{-1}$
Specific heat, C	859 $J.kg^{-1}.K^{-1}$
Density, ρ	1610 $kg.m^{-3}$

Table 1 Mechanical and thermal properties of CFRTP unidirectional ply

In the present study, the infrared thermography technique was adapted, using Ω_{fiss} as a line normal to the fracture propagation direction (Figure 5), denoting t_A and t_{A+dA} respectively the instant just before and just after the crack crossing this line. Critical energy release rate was then evaluated as shown in equations (3) and (4). In each sample, several lines were placed to capture G_{IIC} values evolution along the crack length as shown in Figure 5. The mean value of G_{IIC} of these lines is shown in Table 2 for static and dynamic samples. These values are in agreement with the reported data but the same scatter found in literature can be observed considering present results. There is no significant difference between G_{IIC} for quasi-static and dynamic tests because in both cases mode II delamination is unstable. The crack growth velocity was very high and independent from loading rate.

In fact, the infrared camera frame rate did not allow following the crack tip propagation since crack lengths were small (1-3 mm). In dynamic test D1, the maximum frequency allowing the observation of the central part of the specimen is set at 2176 Hz. In Figure 6(a) the origin in time (t=0) is right before the crack propagation. When the crack crosses a line (Ω_{fiss}), G_{IIC} rises. One can see that crack crosses every line at the same moment and one frame after the origin (t=1/2176~0.0005s). Afterwards, G_{IIC} decreases softly due to dissipative phenomena.

Figure 6(b) shows the evolution of G_{IIC} with the crack length. Even though crack length was small and unstable, delamination is not able to fully develop, a decrease of G_{IIC} can be observed. The energy needed to initiate propagation is higher than the energy needed to keep the crack propagating. This effect has already been proved by [9][10].

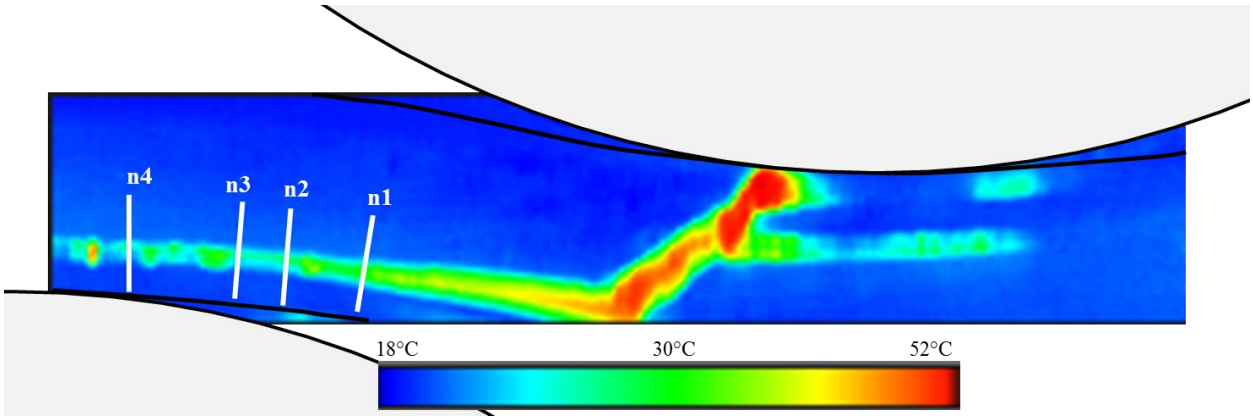

Figure 5 Temperature field during crack propagation for D1 sample

	S1	S2	S3	S4	S5	S6	S7	S8
G_{IIC} (N/mm)	1.22	1.03	1.6	0.92	0.90	1.45	1.42	1.02

	D1	D2	D3	D4
G_{IIC} (N/mm)	1.25	1.63	1.28	1.73

Table 2 G_{IIC} values for quasi-static (S) and dynamic (D) loading samples

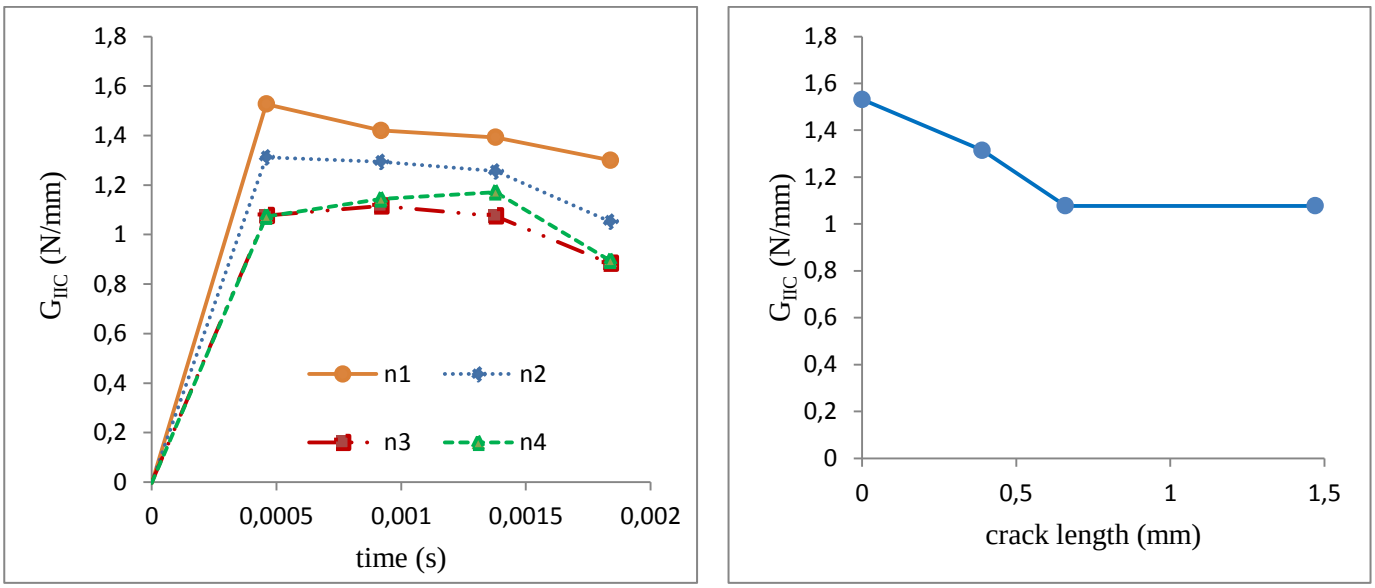

(a) (b)

Figure 6 G_{IIC} versus time for D1 sample (a) and G_{IIC} versus crack length for D1 sample

4 CONCLUSION

In this study, an original experimental test was proposed to identify the critical energy release rate for mode II delamination propagation, G_{IIC}. This parameter is needed to simulate delamination propagation using cohesive zone model under low velocity impact. Short Beam Shear test was retained in order to reproduce impact damage chronology (matrix cracking followed by unstable mode II delamination propagation). Post-mortem micrographies were made in order to confirm this damage scenario. Shear stress state was validated using digital image correlation. Two different loading rates were used: quasi-static (0.4 mm/min) and dynamic (~1m/s). Infrared thermography is a local technique showing good ability to evaluate G_{IIC} for high unstable crack growth during SBS tests. Both loading rates caused similar damage scenario and there was no influence of this loading rate in G_{IIC} values. G_{IIC} values are comprised between 0.9 and 1.7 N/mm. A strong correlation is shown between the values obtained in this study and values found in the literature. More study is needed to fully understand the nature of the scatter of this result.

Acknowledgment

The authors wish to thank 'Direction Générale de l'Armement' for the funding of this project.

5 REFERENCES

[1] G. Dorey, S.M. Bishop, and P.T. Curtis. "On the impact performance of carbon fibre laminates with epoxy and PEEK matrices". *Composites Science and Technology*, 23(3):221–237, 1985.

[2] C. Bouvet, S. Rivallant, and J. J. Barrau. "Low velocity impact modeling in composite laminates capturing permanent indentation." *Composites Science and Technology*, 72(16):1977–1988, 2012.

[3] S. Rivallant, C. Bouvet, and N. Hongkarnjanakul. "Failure analysis of CFRP laminates subjected to compression after impact: FE simulation using discrete interface elements". *Composites Part A*, 55:83–93, 2013.

[4] P. Garcia Perez, F. Dau, C. Bouvet and P. Peres. "Low velocity impact on laminate composite with thermoplastic resin", *Proceedings of the International Conference on Dynamics of Composite Structures*, Arles (France), 2015.

[5] Davies P, Sims GD, Blackman BRK, Brunner AJ, Kageyama K, Hojo M, et al. "Comparison of test configurations for determination of mode II interlaminar fracture toughness: results from international collaborative test program". *Plastics, Rubber Comp* 1999;28:432–7.

[6] A.J. Russell and K.N. Street, in "*Toughened Composites"*, ASTM STP 937 (1987) 275-294.

[7] Chai, H. (1990). "Interlaminar shear fracture of laminated composites." *International Journal of Fracture*, 43(2), 117–131.

[8] Pereira, A. B., de Morais, A. B., Marques, A. T., & de Castro, P. T. (2004). "Mode II interlaminar fracture of carbon/epoxy multidirectional laminates." *Composites Science and Technology*, 64(10–11), 1653–1659.

[9] Friedrich K, Walter R, Carlsson LA, Smiley AJ, Gillepsie JW. "Mechanisms for rate effects on interlaminar fracture toughness of carbon/epoxy and carbon/peek composites." *Journal of Materials Science*. 1989, 24(9): 3387-3398.

[10] Smiley AJ and Pipes RB. "Rate sensitivity of mode II interlaminar fracture toughness in graphite/epoxy and graphite/peek composite materials." *Composite Science and Technology*. 1987, 29:1-15.

[11] Allix, O., Ladevéze, P., & Corigliano, A. (1995). "Damage analysis of interlaminar fracture specimens." *Composite Structures*, 31(1), 61–74.

[12] N. Hongkarnjanakul, S. Rivallant, C. Bouvet, and A. Miranda. "Permanent indentation characterization for low-velocity impact modelling using three-point bending test." *Journal of Composite Materials*, 48(20):2441–2454, August 2013.

[13] Lisle, T., Bouvet, C., Pastor, M. L., Margueres, P., & Prieto Corral, R. (2013). "Damage analysis and fracture toughness evaluation in a thin woven composite laminate under static tension using infrared thermography." *Composites Part A*, 53.

[14] Lisle, T., Bouvet, C., Hongkarnjanakul, N., Pastor, M.-L., Rivallant, S., & Margueres, P. (2015). "Measure of fracture toughness of compressive fiber failure in composite structures using infrared thermography." *Composites Science and Technology*, 112, 22–33.

[15] D.F. Adams and E.Q. Lewis. "Experimental study of three and four-point shear test specimens". *Journal of Composites Technology and Research* 17(4):341-349. October 1995

[16] Taylor GI, Quinney H. "The Latent Energy Remaining in a Metal after Cold Working", *Royal Society A: Math., Phys. Eng. Sci*. 1934.